České vysoké učení technické v Praze, Fakulta elektrotechnická

Czech Technical University in Prague, Faculty of Electrical Engineering

Doc. Ing. Pavel Hazdra, CSc.

Řízení rekombinace elektronů a děr v moderních polovodičových strukturách

Control of Electron-Hole Recombination in Modern Semiconductor Devices

Summary

Control of charge carrier recombination and generation in semiconductor structures is an essential part of the semiconductor technology development. Thesis of this lecture is focused on the summary of latest development and trends in two fields where the control of carrier recombination is currently subject of intensive research. Firstly, it is the lifetime control in high-power silicon devices and, secondly, the application of nanometric InAs/GaAs quantum coupled structures for control of radiative recombination in the near infrared band. The lecture is based on the results, which were achieved in laboratories of the Department of Microelectronics, Faculty of Electrical Engineering, Czech Technical University in Prague in cooperation with Czech and foreign academic and industrial partners, and introduces them in the wider international context.

Irradiation by electrons, protons or alphas allows an accurate and localized introduction of lattice defects acting as recombination centers. In this way, carrier lifetime can be killed only in that part of semiconductor device where it is necessary. This is indispensable in the case of high-power bipolar devices where an appropriate control of the electron-hole plasma collapse during the reverse-recovery reduces the turn-off losses and extends the safe operating area of the irradiated device. Different irradiation techniques are compared from the point of view of introduced recombination centers, their distribution and thermal stability. Optimum axial lifetime structuring in the power P-i-N diode for optimization of the trade-off between on-state and off-state losses is presented. Negative side-effects given by irradiation and means of their elimination are also discussed. Finally, lifetime killing by in-diffusion of platinum (palladium) guided by radiation defects introduced by helium irradiation is presented. This technique allows introducing an arbitrary profile of ideal recombination centers and optimizing the doping profile of the device.

Quantum confinement of electrons and holes in semiconductor nanostructures into regions comparable with their de Broglie wavelength (~ 0.1 - 10 nm) allows to set the transition energy and significantly enhance the intensity of radiative recombination. For this reason, InAs/GaAs quantum wells or dots can be advantageously used as an active layer of highly-efficient and stable lasers operating in the 1.3 or 1.55 μm optical communication band. Characterization of these InAs nanostructures grown on GaAs by metalorganic vapor phase expitaxy is presented and the application of the numeric simulation for identification of electronic transitions is demonstrated. Finally, the effect of quantum dot covering by InGaAs (GaAsSb) strain reducing layer is discussed regarding its influence on the morphology of quantum dots and their electronic states.

Souhrn

Řízení procesů rekombinace a generace nositelů náboje v polovodičových strukturách tvoří neodmyslitelnou součást rozvoje polovodičové elektroniky. Teze této přednášky se zaměřují na shrnutí nejnovější poznatků a trendů ve dvou oblastech, ve kterých je v současnosti ovládání rekombinace nositelů náboje předmětem intenzivního výzkumu. Jedná se o řízení doby života nositelů náboje ve vysokovýkonových křemíkových součástkách a využití nanometrických kvantově vázaných struktur systému InAs/GaAs pro ovládání zářivé rekombinace v blízkém infračerveném pásmu. Přednáška prezentuje především ty výsledky, které vznikly v laboratořích katedry mikroelektroniky Elektrotechnické fakulty Českého vysokého učení technického v Praze ve spolupráci s tuzemskými a zahraničními akademickými i průmyslovými partnery, a uvádí je do širšího, mezinárodního kontextu.

Ozáření energetickými částicemi (elektrony, protony a alfa částicemi) je významným nástrojem pro přesné a lokalizované zanášení krystalových poruch do té oblasti polovodičové struktury, kde je nutné snížit dobu života nadbytečných nositelů náboje. To je nezbytné zejména u vysokovýkonových bipolárních křemíkových součástek pro řízení extrakce elektron-děrové plazmy během jejich závěrného zotavení. Cílem je především snížení vypínacích ztrát a rozšíření oblasti bezpečné činnosti. Vhodnost jednotlivých ozařovacích technik je porovnána z hlediska parametrů zanášených rekombinačních center, jejich profilů a stability. Diskutovány jsou nežádoucí vlivy spojené s ozářením a možnosti jejich odstranění, způsoby vzájemné optimalizace statických a dynamických výkonové P-i-N diody axiálním strukturováním doby života. Dále je popsáno využití iontového ozáření pro řízení difúze platiny a paladia, které umožňuje lokální zanášení ideálních rekombinačních center s vysokou teplotní stabilitou a vhodné nastavení dotačního profilu součástky.

Polovodičové nanostruktury omezující pohyb elektronů do oblastí srovnatelných s jejich vlnovou délkou (~ 0.1 – 10 nm) významným způsobem ovlivňují energii a účinnost zářivých přechodů v polovodičových strukturách. Kvantové jámy či tečky systému InAs/GaAs jsou proto perspektivní pro konstrukci výkonných a stabilních laserů pro optická telekomunikační pásma 1.3 a 1.55 μm. Prezentována je problematika charakterizace těchto InAs nanostruktur vypěstovaných v GaAs metodou plynné epitaxe z organokovů. Demonstrován je význam numerické simulace pro identifikaci kvantových přechodů a naměřených dat. V závěru je diskutován vliv překrytí InGaAs (GaAsSb) vrstvou redukující pnutí na morfologii kvantových teček a jejich elektronové stavy.

Klíčová slova: polovodiče, rekombinace, hluboké úrovně, řízení doby života, výkonové diody, radiační poruchy, ozáření, ionty, elektrony, radiací zvýšená difúze, protony, částice alfa, křemík, platina, paladium, kvantové tečky, kvantové jámy, plynná epitaxe z organokovových sloučenin, optické vlastnosti, elektronové stavy, fotoluminescence, fotomodulovaná reflexe, arzenid india, arzenid galia.

Keywords: semiconductors, recombination, deep levels, lifetime control, power diodes, radiation defects, irradiation, ions, electrons, radiation enhanced diffusion, protons, alphas, silicon, platinum, palladium, quantum dots, quantum wells, metalorganic vapour phase epitaxy, optical properties, electron states, photoluminescence, photomodulated reflectance, indium arsenide, gallium arsenide.

CONTENTS

1. Introduction

Improvement of semiconductor materials or devices performance necessitates a precise control of processes leading to recombination or generation of charge carriers. In semiconductors, electrons and holes can be created or annihilated by different mechanisms which are classified according to the ways in which the energy is released when nonequilibrium carriers leave their bands. There are three basic recombination mechanisms: nonradiative recombination, band-to-band radiative recombination, and Auger band-to-band recombination. The relative importance of the particular mechanism depends on the width of the bandgap and its structure, on the electron and hole densities, presence of recombination centers, etc.

In an indirect band semiconductor like silicon, the change of the electron momentum is necessary and the nonradiative recombination prevails. The recombination is controlled by recombination centers exhibiting deep levels in the semiconductor bandgap and the energy of the recombining carriers is released via phonon emission. Deep-levels arise from crystal defects or impurities introduced during fabrication process. Control of non-radiative recombination has a key importance in bipolar devices, radiation detectors or silicon solar cells. In high-power silicon bipolar devices, the axial/lateral control of carrier lifetime by recombination centers introduced by different irradiation techniques allowed a significant reduction of turn-off losses and extending the safe operating area. This topic is thoroughly discussed in the first part of the lecture.

In direct band semiconductors, no change of electron momentum is necessary and the excess energy of recombining electron-hole pair is released by emission of photon. Radiative recombination is mainly exploited in semiconductor light sources. Quantum confinement of holes and electrons in semiconductor nanostructures allows to tune transition energy and significantly enhance intensity of radiative recombination. This will shown in the second part on the example of InAs/GaAs quantum wells and dots investigated as a prospective active layers for highly-efficient and stable lasers for the 1.55 μm optical communication band.

Results presented were achieved at the Department of Microelectronics, Czech Technical University in Prague in cooperation with numerous academic and industrial partners. In the field of advanced lifetime control in high-power devices an intensive cooperation has been ongoing with Institute of Nuclear Physics ASCR, Forschungzentrum Dresden, Ruhr Universität Bochum, IPF Dresden, CNM Barcelona, Semiconductors, Prague Inc., ABB Switzerland, Semiconductors Ltd., etc. Results obtained on InAs/GaAs nanostructures then originate from a fruitful cooperation with the MOVPE group of the Institute of Physics ASCR.

2. Control of Non-Radiative Recombination in Power Devices

In recent years, the irradiation with fast electrons and ions became a dominant technique for an accurate control of carrier lifetime in silicon power devices. Radiation defects, which can be precisely placed in different location of the device (see Fig.1), are introduced to enhance the recombination of excess carriers, decrease the switching time and turn-off energy losses (see Fig.2) [1]. First, the electron irradiation with energies from 1.5 to 12 MeV, which guarantees an axially homogeneous distribution of recombination centers in up to 1000 μm thick power devices, substituted the traditional methods of lifetime killing based on the noble metal (platinum, gold) diffusion. This technique profited from its uniformity, controllability and productivity [3]. Latterly, the irradiation with high-energy protons and alphas came to be popular since it allows an introduction of a very narrow defect region where the carrier recombination is enhanced [4]. By choosing an appropriate energy of the projectile, this region with locally reduced lifetime can be precisely placed only in that part of the device, where it is necessary. Switching parameters of ion irradiated devices are then improved without serious deterioration of static ones [5]. Moreover, multiple ion irradiation can introduce complex, custom-specific profiles of recombination centers to further optimize device characteristics and extend its safe operation area [1]. Attention also turned to the application of electron irradiation with energies lower than 1 MeV [2]. In this case, the full-width half maximum (FWHM) of the absorbed dose distribution is comparable to the device thickness. This allows introducing so-called “sloping” profile giving a gradual decrease of the defect

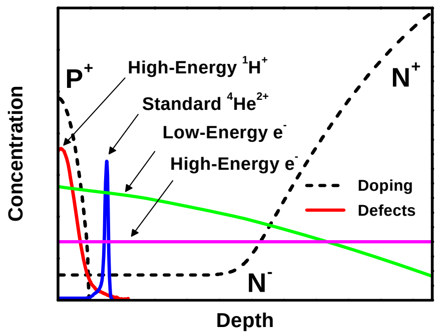

Fig.1 Doping profile of power P-i-N diode with measured concentration profiles of recombination centers – homogeneous (high energy electrons), local (standard alphas), sloping sharp (high-energy protons) and gradual (low-energy electrons) [2].

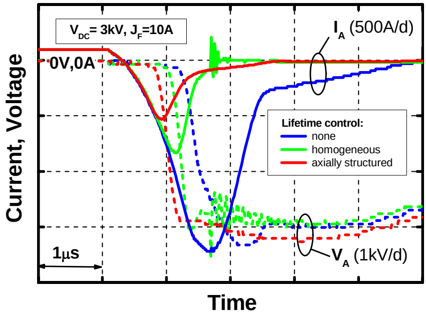

Fig.2 Reverse recovery waveforms of the P-i-N diode subjected to different lifetime killing – none, homogeneous (electron irradiation) and axially structured (ion and electron irradiation). Advanced lifetime killing reduces reverse recovery charge and increase diode softness.

concentration from the irradiated surface up to a certain depth in the device. Sharper slopes can be also achieved by high-energy proton irradiation through appropriate set of energy degraders (foils) [2].

When strong lifetime reduction is required, application of irradiation methods brings undesirable increase of leakage and parasitic doping which can decrease device blocking capability [6]. Proper post-irradiation annealing usually reduces leakage problems, but it can simultaneously enhance negative doping effects. It was shown that these drawbacks can be avoided when radiation damage is used for guiding the in-diffusion of impurities exhibiting superior recombination properties (platinum, palladium). In this way, an arbitrary profile of ideal recombination centers can be created and superior device parameters can be achieved [7-9].

2.1. Recombination Centers Produced in Silicon by Ion and Electron Irradiation

During silicon irradiation, energetic particles are loosing their kinetic energy by collisions with silicon atoms creating primary damage - vacancies and interstitials. Ions create most of the lattice damage towards the end of their range, enabling localization of the region with high defect concentration while most of the silicon bulk is left relatively unaffected. Lighter electrons have a much higher penetration depth and are subjected to larger deflection. As a result, the damage is homogeneous for typical irradiation energies (>1MeV). Primary defects are unstable and interact with each other or with structural imperfections of the target, creating secondary stable defects, mostly vacancy related complexes such as divacancies and vacancy-impurity pairs (e.g. vacancy-phosphorus, vacancy-oxygen, etc.). This process is affected especially by the conditions of irradiation (dose, temperature, dose rate) and subsequent annealing, type of projectile, target material and its thermal history [10]. The radiation defects change the crystal structure locally and give rise to energy levels appearing deeper in the silicon bandgap. The deep levels generated in this way affect non-radiative (thermal) generation and recombination of free carriers and consequently the minority carrier lifetime.

Deep levels influence semiconductor properties even at very low concentrations (~ 0.01 ppb). Deep Level Transient Spectroscopy (DLTS) is a very sensitive method monitoring a transient capacitance response of the pn junction to identify emission rates connected with particular deep levels. Fig.3. shows typical DLTS spectra of majority carrier traps recorded on n-type silicon irradiated with protons, alphas high- and low-energy electrons [2]. Corresponding survey of identified deep levels is then presented in Fig.4. Fig.3 shows that irradiation with electrons and alphas produces pure radiation defects: divacancy – V_2, vacancy-oxygen pair - VO, and carbon-oxygen interstitials pair C_iO_i; giving rise to different deep levels in silicon bandgap. The most prominent of them are the acceptor level of vacancy-oxygen pair $VO^{-/0}$, which is the most efficient recombination center at high injection levels, and the single-acceptor level of divacancy $V_2^{-/0}$, which is responsible for carrier recombination at low injection and generation in the depletion regime. Annealing of divacancies at temperatures above 320˚C results in formation of more stable high-order vacancy complexes which can either influence leakage of irradiated device or can getter other impurities present in the bulk of semiconductor.

DLTS spectrum measured on H^+ implanted sample is richer and shows that hydrogen in contrast with helium interacts with radiation defects and other crystal imperfections giving rise to additional hydrogen related levels. These levels have a negligible influence on carrier generation and recombination due to their low carrier capture cross sections. However, the implanted hydrogen stimulates formation of shallow hydrogen donors (HDs) in the vicinity of its end-of-range. HDs concentration is comparable with the original shallow doping already at proton fluences of 10^{11} cm^{-2}. This can accelerate breakdown of the irradiated device [11].

Fig.2 also presents DLTS spectra recorded on silicon doped by platinum and palladium [7,9]. Substitutional atoms of these impurities exhibit nearly identical electronic properties: a series of deep levels in the silicon band gap: acceptor at E_C-0.23eV($Pt_s^{-/0}$)/E_C-0.22eV($Pd_s^{-/0}$), donor at

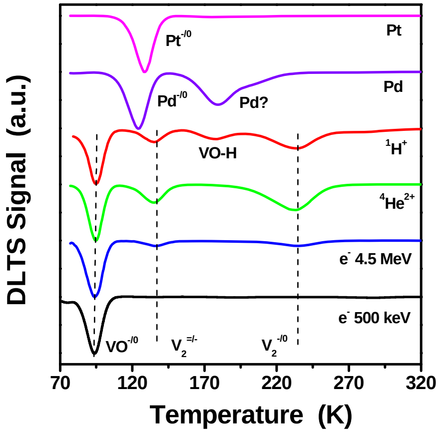

Fig.3 Majority carrier DLTS spectra measured in n-type silicon subjected to different lifetime killing (Pt or Pd in-diffusion, irradiation with protons, alphas high- and low-energy electrons). [2, 7, 9]

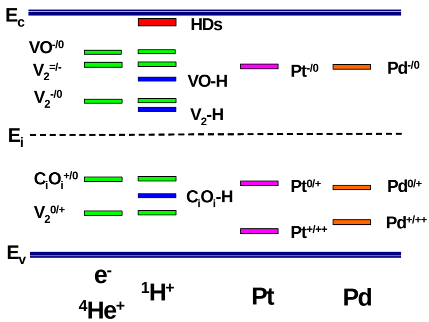

Fig.4 Survey of deep levels appearing in silicon bandgap after different lifetime killing.

E_V+0.32eV($Pt_s^{0/+}$)/E_V+0.33eV($Pd_s^{0/+}$) and double-donor at E_V+0.13eV ($Pt_s^{+/2+}$)/E_V+0.17eV($Pd_s^{+/2+}$) – see Fig.4. Since the acceptor level of Pt_s(Pd_s) is nearly an ideal recombination center, lifetime killing by platinum/palladium is, from the point of view of the introduced levels, superior to radiation treatment. The in-diffusion of Pt(Pd) also does not increase device leakage because since no levels are located close to the middle of silicon bandgap. However, the technique lacks of controllability.

Detailed knowledge about radiation defect distribution is a must for their application in lifetime tailoring. Fig.5 shows a typical example of

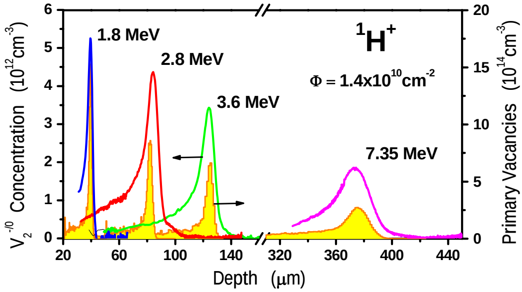

Fig.5 Concentration profile of the single acceptor level of divacancy in silicon irradiated with 1.8, 2.8, 3.6 and 7.35 MeV protons to a fluence of 1.4×10^{10} cm^{-2} measured by the reverse I-V profiling (thick). The simulated distributions of primary vacancies are also shown.

concentration profiles of radiation defects resulting from ion irradiation - distributions of the single-acceptor level of the divacancy $V_2^{(-/0)}$ in silicon irradiated with 1.8, 2.8, 3.6 and 7.35 MeV protons to a fluence of 1.4×10^{10} cm^{-2} [12]. The profiles were obtained by I-V profiling, the newly developed method for non-destructive characterization of radiation defect profiles in the full depth of power devices [13]. The method traces the gradient of the reverse current of the irradiated device versus the depth of the space charge region (SCR) *dI/dx* which is a measure of divacancy distribution. Fig.5 shows that divacancy distribution follows well that of the primary damage only with a small broadening due to vacancy diffusion which is necessary for formation of secondary stable defects. Similar results were obtained for other recombination centers in silicon irradiated by protons and alphas. Detailed information about defect introduction rates can be found in [12].

To be applied in semiconductor device technology, radiation defects have to be thermally stable at operation temperature of given device. For this reason, irradiated devices are usually annealed at temperatures ranging from 200 to 350ºC. In helium irradiated silicon, annealing at 220ºC does not affect VO pairs while divacancies anneals out with formation of a new centre with two charge states located close to $V_2^{-/0}$ and $V_2^{=/-}$. The new centre, which starts to form at 220ºC and anneals out at 325-350ºC was identified as V_2O complex. This complex, which is formed by reaction of divacancies with interstitial oxygen according to the reaction $V_2+O_i \rightarrow V_2O$, is responsible for faster annealing of divacanies in oxygen rich silicon. Above 350°C, the annealing of VO and V_2O gives rise to multiple vacancy V_n and VO_n complexes. For low irradiation fluences, these centers remain strongly localized close to the alpha's range up to 430°C and kill carrier lifetime significantly [11].

In contrast with helium, annealing of radiation damage in proton irradiated samples is influenced both by the presence of interstitial oxygen and implanted hydrogen. Recent investigations performed on hydrogenated, electron irradiated silicon show, that interaction of divacancies with hydrogen takes place at higher rate than with oxygen [14]. This results in disappearance of V_2 without a corresponding formation of V_2O or other electrically active centre. The proposed interaction is the direct formation of V_2H_2 complex according to the reaction $V_2 + H_2 \rightarrow V_2H_2$ without formation of the intermediate, electrically active V_2H centre. Hydrogen also affects annealing of VO pair, which is normally stable up to $\geq 350°C$ (in the absence of hydrogen). In samples containing hydrogen, it anneals between 275 and 300°C by transformation to VOH centre $VO + H \rightarrow VOH$. This centre subsequently anneals out by a capture of a second hydrogen atom with formation of electrically inactive VOH_2 defect. Also in proton irradiated samples, the annealing of V_2O, VO and VOH above 350°C is accompanied by formation of new centers (identical to those observed in helium irradiated silicon) which reduce lifetime and remain localized at the radiation damage peak [11].

2.2. Radiation Defects and Formation of Shallow Donors

Favorable effect of ion irradiation can be accompanied by negative side effect - parasitic doping. This effect is important for power devices which are usually produced on high resistive n-type silicon to provide high blocking voltages. Therefore, device blocking capability can be easily lost when an additional donor doping caused by the radiation damage is placed into the highly resistive region of the device. This is the case of proton irradiation followed by low-temperature ($< 400°C$) annealing (necessary for defect stabilization), when formation of shallow donor levels related to hydrogen-defect complexes is enhanced [15].

For a long time, helium irradiation was considered to be free of donor doping side-effects. However, the post-irradiation annealing at temperatures above 350°C, which is required for increasing of radiation defect stability or soldering of irradiated devices into modules, discovered that helium irradiation also introduces shallow donors which follow the profile of radiation damage produced by helium ions (see Fig.6a). This is taking place in oxygen-rich silicon irradiated with helium ions which is annealed in air at temperatures from 350 to 500ºC. Origin and evolution of these radiation enhanced thermal donors (RETDs) is moderated by hydrogen atoms diffusing from anode contact into silicon bulk (see Fig.6b). Hydrogen stimulates diffusion of oxygen interstitials (O_i) and allows them to react with VO pairs. Possible scenario is the enhanced generation of VO_2 centers by reaction $VO + O_i \rightarrow VO_2$ with subsequent formation of oxygen dimers O_{2i} ($Si_i + VO_2 \rightarrow O_{2i}$) what is the first step of oxygen agglomeration preceding TD formation. Therefore, the origin of RETDs in silicon is conditioned by simultaneous presence of hydrogen, interstitial oxygen and radiation defects containing vacancies and oxygen. At higher irradiation fluences or in the peak of radiation damage, concentration these centers and, consequently, RETDs growth saturates. As a result, profiles of RETDs are broader and flatter [16].

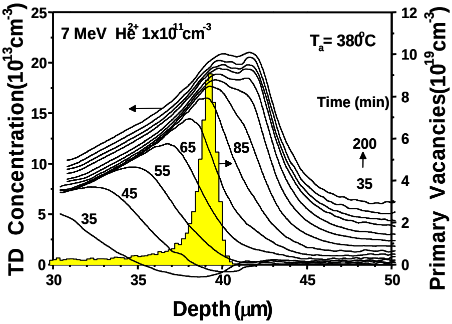

Fig.6a Evolution of the excess donors in FZ oxygen-rich silicon irradiated with 7 MeV alphas to a fluence of $1x10^{11}$ cm^{-2} during isothermal annealing on air at 380ºC. The simulated profile of primary defects (vacancies) also is shown for reference.

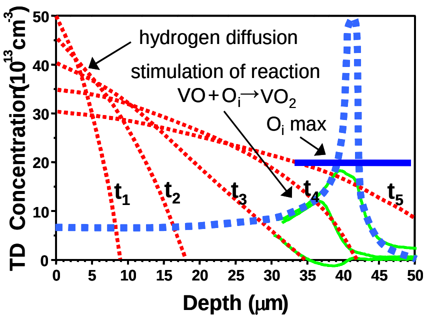

Fig.6b Model explaining RETD formation by diffusion of hydrogen which stimulates formation of RETD cores (VO_2 centers). The reaction is limited by the maximum concentration of oxygen interstitials (O_i).

2.3. Optimization of Power Device Parameters by Advanced Lifetime Killing

Proper lifetime killing in the power device brings a significant improvement of its dynamic parameters like turn-OFF time and turn-OFF losses and enlargement of the safe operating area (SOA). Unfortunately, the improvement of the dynamic parameters is off-set by a worsening of static ones like forward voltage drop (ON-state losses), leakage current (OFF-state losses) and/or blocking voltage. Therefore, any lifetime control technique is attributed to the above mentioned trade-off between the static and dynamic parameters and their mutual optimization is necessary. Development of simulation tools for advanced lifetime killing by irradiation techniques [15,17] allowed a significant process in this field. The impact of different lifetime killing on static and dynamic parameters was then

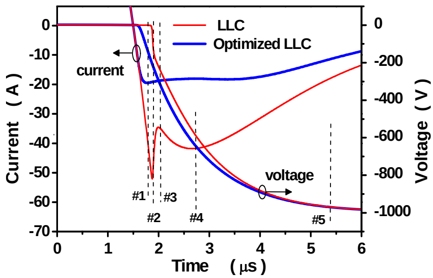

Fig.7a Simulated reverse recovery waveforms of diodes subjected to local lifetime control (LLC) and optimized LLC (single- vs. double-irradiation). Diodes have identical ON-state losses.

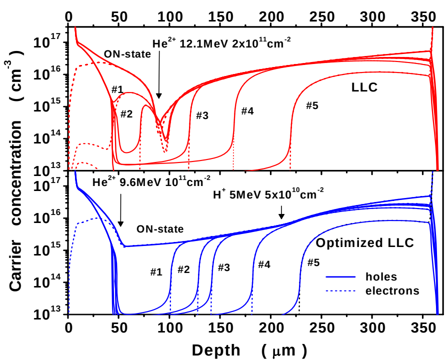

Fig.7b Simulated carrier profiles in at different time instants of the reverse recovery waveforms from Fig.7a.

thoroughly investigated both by simulation and experiment [5,6,18-23]. In power P-i-N structure, reduction of the lifetime and consequently a decrease of the ON-state carrier modulation always increases the forward voltage drop V_F . The only reasonable way of ON-state losses optimization is a precise setting of the axial lifetime profile. This must suppress the electron-hole plasma concentration only where it is necessary and, at the same time, guarantee that the conditions of high-level injection will not be violated. Both conditions can be kept, if the principal lifetime reduction is performed in the anode area. Decrease of the blocking capability is a crucial problem of local lifetime control performed by ion irradiation since the optimum position of the principal damage peak is in the anode junction. Optimum is to keep the damage outside the SCR, if possible. Higher doses of protons ($>10^{11}$ cm^{-2}) must be avoided, if the defect peak location approaches the n-base side of the junction. An additional proton irradiation located in the n-base is not a problem, because it only needs a low proton dose ($<10^{11}$ cm^{-2}). Regarding the dynamic characteristics, the optimum position of the damage layer for simple local lifetime control is close to the anode junction. Turn-off losses and the probability of dynamic avalanche can be further suppressed, if the second damage layer is created deeper in the N-base (see Fig.7). This approach, which decreases the excess carrier concentration only in the left half of the diode, is preferred over the combination of local and uniform lifetime control by electrons since it leaves the charge accumulated at the cathode untouched and therefore ensures softer recovery [1]. Multiple ion irradiation can be performed in one step using a properly designed mask which is inserted between the ion source and the device [24]. Lifetime profile is then shaped by density and structure of the mask. The technique is fully capable to replace multiple ion irradiation and guarantee superior diode performance.

2.4. Lifetime Killing by Diffusion of Noble Metals Controlled by Radiation Defects

In the last two decades, the lifetime killing by gold or platinum in-diffusion was outperformed by irradiation techniques. However, radiation defects anneal-out at relatively low temperatures (~350°C) and they are not ideal recombination centers: in high concentrations, they increase device leakage and cause parasitic doping [11]. On the contrary, in-diffused platinum (or palladium) atoms at substitutional position in silicon lattice Pt_s (Pd_s) are ideal recombination centers, but shaping of their profile is difficult. Combination of both approaches, i.e., application of radiation damage to guide the in-diffusion of noble metals is one possibility how to get an arbitrary profile of ideal recombination centers.

Palladium and platinum atoms behave similarly in silicon. Both can occupy either interstitial, or substitutional site in silicon lattice and their diffusion proceeds via a small fraction of solutes being in the interstitial configuration. In substitutional position, they show similar electronic properties. On the other hand, the solid solubility of active palladium in silicon is 20 to 50 times lower than that of platinum and Pd_s concentration increases more gradually with diffusion temperature. The interchange of interstitial and substitutional Pt (Pd) atoms proceeds in two ways: via the Frank-Turnbull mechanism, which assumes the interstitial impurity X_i to recombine with a lattice vacancy V to a substitutional X_s ($X_i + V \Leftrightarrow X_s$), or using the so-called kick-out mechanism where an interstitial impurity generates a silicon self-interstitial I when occupying a substitutional site ($X_i \Leftrightarrow X_s + I$) [26]. Both the reactions are affected by the number of lattice defects and therefore the diffusion of Pt and Pd can be guided by their artificial introduction, e.g. by irradiation.

Recent investigation showed that the high-energy implantation of helium produces radiation damage which is optimal to guide and localize in-diffusing platinum and palladium atoms (see Fig.8) [8,25,27]. Despite similar chemical and electronic properties, the radiation enhanced diffusion of platinum and palladium exhibits differences. Palladium, in contrast with platinum, in-diffuses already at lower temperatures (<600°C) and introduces substantially higher concentration of recombination centers. This offers higher lifetime reduction and better control of the amount of electrically active recombination centers by selecting a proper annealing temperature. Moreover, deep acceptor levels connected with the low-temperature Pd in-diffusion allow advanced modification of the shallow doping profile in

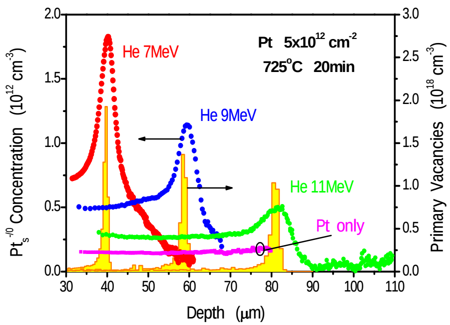

Fig.8 Concentration versus depth profiles of the $Pt_s^{-/0}$ level measured in diodes where the diffusion of platinum (725 C 20 min) was enhanced by implantation of helium ions with energies: 7 MeV, 9, and 11 MeV. The $Pt_s^{-/0}$ profile measured in the diode not implanted with helium is shown for reference [25].

the N-base where the electric field peaks. This is an additional way to suppress the dynamic avalanche and increase the breakdown voltage in any P-i-N diode [8]. Both processes were successfully applied to the local lifetime control in high power silicon diodes and outperformed the standard irradiation techniques in defect stability, leakage and device ruggedness [7].

3. Radiative Recombination in Semiconductor Nanostructures

The strength of an optical transition is given namely by two factors, the density of states, i.e., the number of possible electron-hole transitions at given photon energy, and the dipole matrix element which couples light to the material via a transition of an electron between two states in the conduction and valence band. The transition is stronger for a larger overlap between the electron and hole state and their larger extent.

In a bulk, direct band semiconductor, the transition energy is given by its bandgap and the density of states D(E) is zero at band edges and then increases with the square root of the energy E (see Fig.9). Quantum confinement of electrons and holes in semiconductor nanostructures into regions comparable with their de Broglie wavelength allows to tune the transition energy and significantly enhance the intensity of radiative recombination. Semiconductor nanostructures can be classified according number of dimensions in which the carriers are free to move: 0D quantum dots (QD), 1D quantum wires, and 2D quantum wells (QW). Confinement is usually achieved by embedding the semiconductor with lower bandgap

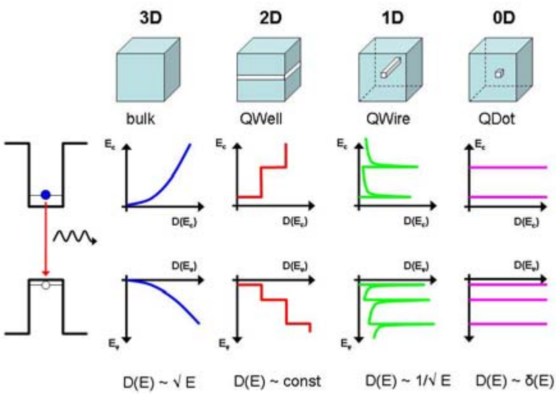

Fig.9 Schematic representation of three-, two-, one- and zero-dimensional heterostructures (top). Densities of electronic states for the given case of dimensionality (bottom).

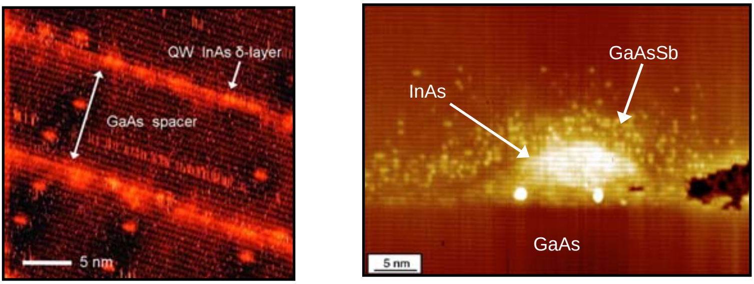

(a) **(b)**

Fig.10 (a) XSTM image of two MOVPE grown InAs ultrathin QWs separated by the GaAs spacer [31]. (b) XSTM image of InAs/GaAs QD capped with GaAsSb [39]. Images were recorded with atomic resolution.

into the matrix of semiconductor with higher one, e.g., InAs into GaAs. An example is shown in Fig.10 where cross sectional scanning tunneling microscopy (XSTM) images of InAs/GaAs QW(a) and QD(a) are presented. When confinement is increased, the bulk density of states splits to subbands (QW) up to discrete states (QD) and the density of states increases significantly. The lowest energy transition is no longer given by the energy gap of the smaller bandgap semiconductor, but increases to the difference between the lowest energy state in the conduction and valence band, resp. This difference, i.e., emission wavelength, can be tuned by dimensions of the nanostructure. Confinement localizes electrons and holes to the same region and increases electron-hole overlap. This leads to larger dipole matrix elements providing higher transition rates.

The most common way for preparation of 2D nanostructures is the growth of heterostructures by epitaxial techniques like molecular beam expitaxy (MBE) or metalorganic vapor phase epitaxy (MOVPE) [28]. Confinement to smaller dimensions was then first achieved by top-down (etch/litographic) methods, however, bottom-up fabrication of quantum dots or wires directly from quantum well structures is taking over by now. Elegant way for making QDs by self-organization is based on the natural tendency of a strained, heteroepitaxial film to roughen, in some cases by forming 3D islands. The process, known as Stranski-Krastanov growth mode [29], is based on the competition between strain and surface energy when a thin "wetting" layer (InAs) is deposited on a substrate with lower lattice parameter (GaAs). Although the growth of the layer is favored initially, the built-up of strain energy makes subsequent layer growth unfavorable, the layer roughens and forms 3D islands (InAs QDs). Increased surface energy of QD is compensated by relaxation of the strain.

3.1. Electronic States in Semiconductor Quantum Wells and Dots

Optical characterization methods like photoluminescence (PL), photocurrent absorption (PC) and photomodulated reflectance (PR) spectroscopy offer fast, non destructive and contactless means for identification of electronic states in nanostructures [28,29]. However, correct interpretation of measured data has to be supported by simulation of electronic states in QD structures. Nowadays, this can be done by a proper 3D simulator. An example is **nextnano3** [30] where the computations start for a given nano-structure by globally minimizing the total elastic energy using a conjugate gradient method. This determines the piezo-induced charge distributions, the deformation potentials and band offsets within the nanostructure. Subsequently, the carrier wave functions Ψ_i and energies E_i are calculated by solving iteratively 8-band-Schrödinger and Poisson equations. Since some material or structural parameters are usually unknown, a proper calibration of the simulation is a must.

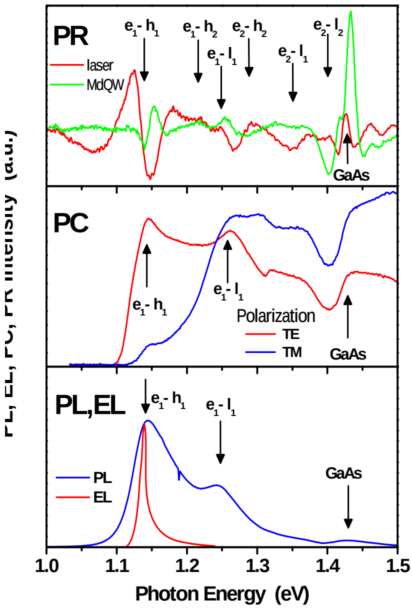

Fig.11 Left: Room temperature photoreflectance (top), photocurrent (middle) and photoluminescence (bottom) spectra of MdQW and semiconductor laser where the identical MdQW was used as an active layer. Theoretical quantum transitions identified by simulation are also indicated.

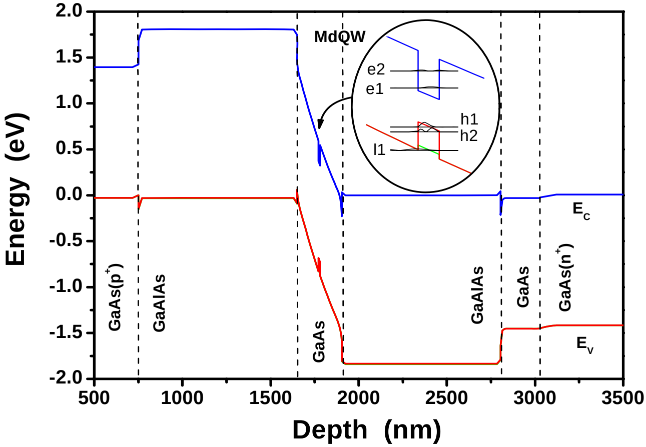

Fig.12 Simulated band structure of the laser structure using the InGaAs MdQW as an active layer. The electronic states and wavefunctions in the MdQW are shown in the inset.

Fig.11 shows a typical example of experimental data obtained by opto-electrical measurement: room temperature PR, PC, and PL spectra recorded on semiconductor quantum structure – modulated InGaAs QW (MdQW) and a semiconductor laser which uses the identical MdQW as an active layer [31]. The upper PR spectrum shows strong resonances corresponding to the optical transitions in the InGaAs MdQW. The arrows indicate the transition energies obtained from fitting the PR data. The notation e_n-$h(l)_m$ denotes the transition between n-th state in conduction subband and m-th heavy hole (light hole) state in valence subband. The identification of particular transitions was done by electronic state simulation. The strongest resonance at lowest energy is attributed to e_1-h_1 transition. Besides it, the PR spectrum shows e_1-l_1 transition – the lowest energy transition for light holes, and transitions between excited states: e_1-h_2, e_2-h_2, e_2-l_2, and e_2-l_1. The optical transitions e_1-h_2 and e_2-l_1 are forbidden, but the built-in electric field in the structure makes them possible to be observed in PR measurement. Two PC spectra measured with TE and TM polarizations (electric vector parallel/perpendicular to the growth direction) allow unambiguously identifying two (e_1-h_1 and e_1-l_1) ground state transitions. Identical transitions can be resolved in the PL spectrum together with the peak attributed to the GaAs band-to-band transition. Electroluminescence (EL) spectrum then confirms that the laser is lasing at the wavelength corresponding to the ground state e_1-h_1 transition. Finally,

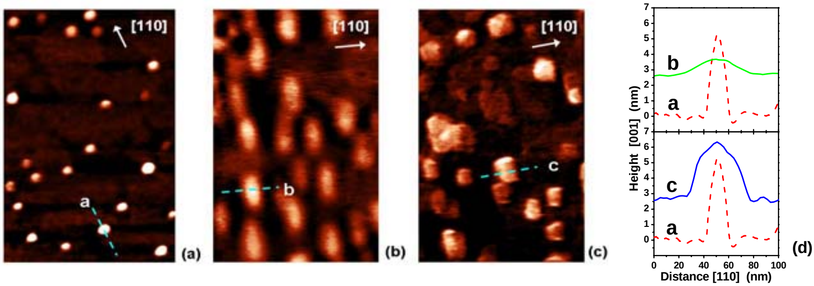

Fig.13 300 nm x 500 nm size AFM image of uncapped InAs QDs (a) and QDs covered with 2.5 nm thick GaAs (b) and $In_{0.23}Ga_{0.77}As$ cap (c) and their cross sections taken along the [110] direction (d).

the model of the full laser structure can be built (see Fig.12) and used for optimization of lasers with different strained InGaAs MdQWs. In our case, this allowed to tune laser wavelength from 890 to 1100 nm and achieve low threshold current density (up to 0.12 kA/cm^2) and high quantum efficiency (up to 35 %) [31].

3.2. Recombination in Self-Assembled InAs Quantum Dots in GaAs

Interest in self-assembled InAs/GaAs quantum dots (QDs) study is motivated by the demand for high-speed, low-power, temperature-stable lasers and detectors for 1.3 or 1.55 µm optical communication bands based on cheap GaAs substrate. Despite a significant success in the fabrication of 1.3 µm QD lasers, achieving emission at 1.55 µm by InAs/GaAs QDs is difficult. The compressive strain energy in the QDs, which increases with QD size, imposes an upper limit on the size of defect free QDs. Similarly, the strain increases with increasing thickness of the capping layer (CL) embedding QDs into a functional structure. Capping of QDs also brings redistribution of In atoms affecting QD size [32]. Therefore, the final optical characteristics of the overgrown QD layers are significantly influenced by the CL growth parameters like its composition, thicknesses, growth temperature and growth rate. Several approaches are used to control the strain field and to increase the QD size, e.g., by introduction of tensile stress by InGaNAs capping layer (CL) [33], by the growth on metamorphic InGaAs buffer [34], and using InGaAs strain reducing layer (SRL) [35].

Fig.13 shows a typical 300x500 nm^2 atomic force microscopy (AFM) image of the uncovered InAs QDs. These QDs were prepared by low-pressure MOVPE on semi-insulating GaAs (001) substrates using the

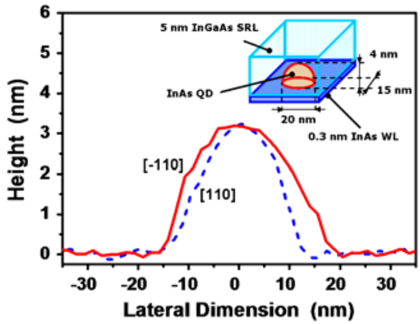

Fig.14 Height profile of a typical InAs QD measured in two ([-110] - solid and [110] - dashed) perpendicular directions (bottom) and corresponding model used for simulation (inset).

Stranski–Krastanow growth mode. The structures were grown at 490°C except the first GaAs buffer layer (650°C). InAs wetting layer was deposited for 27 s with a growth rate of 0.06 monolayer per second. The growth was then interrupted for 15 s to allow QDs formation [36]. Fig.13a shows that the uncovered QDs are InAs lenses which are slightly elongated in the [-110] direction. The average density of QDs is $1.3x10^{10}$ cm^{-2}, lateral dimensions along [-110] and [110] axes are 25±10 and 22±8 nm, resp., and their average height is 4.0±1.3 nm. Example of the typical QD height profile measured by AFM in [110] and [-110] directions is shown in Fig.14. The inset of Fig.14 shows a 3D model of a lens shaped QD which was developed to interpret PL and AFM data [37].

A significant spread of QD sizes causes that the uncovered layer of QDs exhibits a broad PL spectrum which peaks at 1.43 µm (see Fig.15 - dashed). Covering of these dots by 2.5 nm GaAs CL improves homogeneity of QD structure - the PL peak significantly narrows, retains its intensity and spectral position. Further GaAs capping increases the PL intensity and causes a blue shift (up to 1.26 µm) narrowing further the PL peak (Fig.15 left). The blue shift is caused both by the increasing strain in the structure (increases the InAs bandgap) and by the transformation of QDs to elongated InGaAs islands with InAs core (see figure Fig.13b). During GaAs capping, In atoms migrate from the top of QDs and are incorporated into the CL [32]. Dissolution of QDs predominantly decreases the QD height (see the cross sections in the upper part of Fig.13d) and contributes to the blue shift of PL maxima. Migrating In atoms driven by the strain field get embed in the vicinity of the QD and form an InGaAs island around it. The elongation of the island in [-110] direction then is caused by anisotropic lateral growth rate.

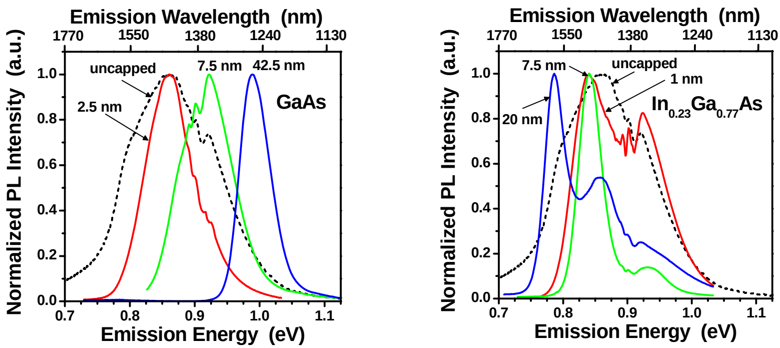

Fig.15 Room temperature PL spectra of InAs QDs covered by 0, 2.5, 7.5 and 42.5 nm thick GaAs CL (left) and 0, 1, 7.5 and 20 nm thick $In_{0.23}Ga_{0.77}As$ SRL (right).

3.2. Influence of Strain Reducing Layer

While GaAs capping does not allow to reach emission at 1.55 μm, a proper $In_{0.23}Ga_{0.77}As$ SRL can shift the emission up to the desired wavelength. Fig.15 (right) shows that increasing $In_{0.23}Ga_{0.77}As$ CL narrows the PL maxima (its full width at half maximum decreases up to 35-50 meV) and causes its red shift. Simultaneously, the energy separation between the ground and first excited state stays within 70 to 80 meV. There are three reasons of this positive effect. Firstly, the InGaAs CL relieves some of the compressive strain in the QD which reduces the InAs bandgap [36]. Secondly, the InGaAs SRL lowers the barrier height on the top of the QD. This reduces quantum confinement, electron wave functions significantly spread into the SRL (see Fig.16) and transition energy lowers [37]. Thirdly, the increasing In content in the SRL decreases the lattice mismatch between the cap and the QD. The chemical potential of In atoms changes and the detachment rate of In atoms and their migration away from the QDs decreases [38]. As a result, the height of larger QDs can be preserved (compare AFM images 13b and 13c and cross sections in figure 13d). Higher In content in the SRL could even increase QD height/size.

Recently [39], the effect of GaAsSb SRL was investigated. In this case, the QD size is preserved but not increased as compared with InGaAs SRL. This results in lower red shift of QD PL (see Fig.17). However, the most important difference between InGaAs and GaAsSb SRLs is in band alignment of structures. The system with InAs QDs covered with

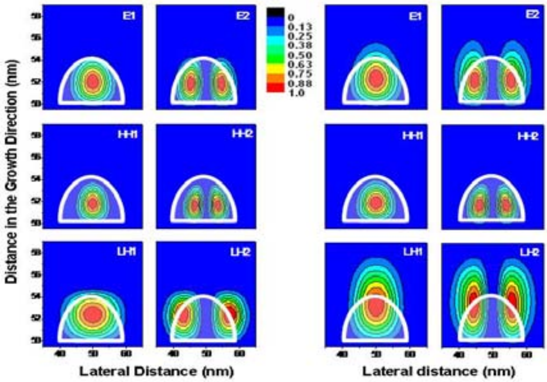

Fig.16 Simulated electron (top), heavy- (middle) and light-hole (bottom) wave function distributions in QDs covered by SRL with 0% (left) and 30% (right) of In concentration - the ground (1) and the first excited state (2). The QD shape is also indicated – cross section along the growth direction.

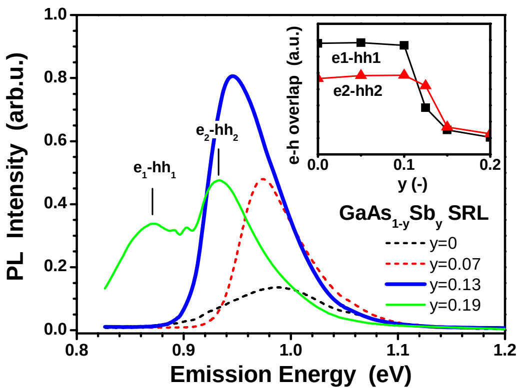

Fig.17 PL spectra of QDs capped by $GaAs_{1-y}Sb_y$ SRL with Sb content y ranging from 0 to 0.19. Inset shows the integral of the product of the density of probability of electron and hole states on the Sb content, where e1-hh1 (squares) is the transition between electron and heavy hole ground states and e2-hh2 (triangles) transition between first excited states.

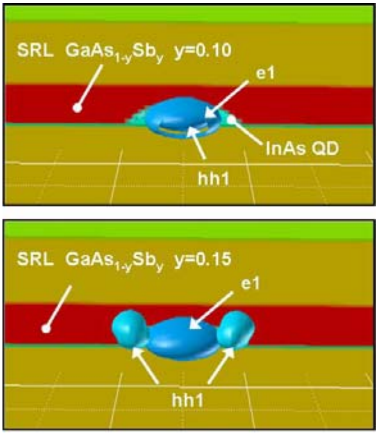

Fig.18 Simulated wave functions of the electron and hole ground states in the InAs QDs covered by $GaAs_{1-y}Sb_y$ SRL for y=0.10 (top) and 0.15 (bottom).

the InGaAs SRL is a pure type I heterojunction while in the system using GaAsSb SRL a type I to type II transition occurs when the Sb content reaches 14%. For structures with a higher Sb content in the SRL, the red shift of QD PL increases considerably, however, the cost for this red shift is lower PL efficiency due to lower overlapping of electron and hole wave functions (see Fig.18) [40]. This is because holes start to be confined in the GaAsSb SRL instead of InAs QD. As a result, PL from the ground states transition (e_1-h_1) ceases and emission from the excited state (e_2-h_2) exhibiting better electron-hole wave function overlap increases (see the inset in Fig.17). Another disadvantage for laser application is the blue shift and broadening of ground state emission with increasing excitation intensity. On the other hand, important advantage of using GaAsSb instead of InGaAs SRL is the possibility to change the localization of holes in the structure by GaAsSb composition. This can increase the oscillator strength and PL intensity of ground state emission. For low Sb concentration holes are localized near the QD base. With increasing Sb concentration the hole wave function centre of gravity shifts towards the QD apex. Fig.17 shows that maximum PL intensity, i.e. the highest overlap of electron and hole wave functions, is achieved for 13% content of Sb in the SRL just before type transition. In addition, only the ground state emission is observed in this case (even for a substantial increase of excitation power). This is an important advantage of GaAsSb covering compared to samples with InGaAs SRLs, where the excited state emission was always observed even at the lowest excitation powers.

4. Conclusions

Latest developments and trends in two fields, where the control of carrier recombination is currently subject of intensive research, were presented.

In the case of the control of non-radiative recombination in high-power bipolar silicon devices, research works focus on the low-temperature, precisely controlled introduction of lattice defects acting as recombination centers. Since the behavior of the modified device is very sensitive to the amount and distribution of lifetime killers, the lifetime control has to be performed with high reproducibility and homogeneity. It was shown that combination of irradiation by electrons, protons or alphas is a proper mean for this purpose. Different irradiation techniques were compared from the point of view of introduced recombination centers, distribution profiles and thermal stability. Optimum axial lifetime structuring in the power P-i-N diode for optimization of the trade-off between on-state and off-state losses was presented. Negative side-effects given by irradiation (parasitic doping, leakage, etc.) and means of their elimination were also discussed. Finally, it was shown that lifetime killing by in-diffusion of platinum (palladium) guided by radiation defects introduced by helium irradiation outperforms standard irradiation techniques in thermal stability of defects, leakage and device ruggedness.

The favorable effect of quantum confinement of electrons and holes in semiconductor nanostructures for enhancement and control of radiative recombination was demonstrated on the case of InAs quantum dots embedded in the GaAs matrix. Characterization of these InAs nanostructures grown on GaAs by metalorganic vapor phase expitaxy was presented and the application of the numeric simulation for identification of electronic transitions was demonstrated, as well. It was shown that a proper covering of InAs quantum dots by InGaAs (GaAsSb) strain reducing layer allows to use them as an active layer of highly-efficient and stable lasers operating in the 1.3 or 1.55 μm optical communication band.

It was shown that any future development in both fields is unconceivable without use, improvement and mutual cooperation of three key factors – technology, diagnostics and device simulation.

References

[1] P. Hazdra, J. Vobecký, K. Brand, Nucl. Instr. Meth. B 186 (2002) 414.

[2] P. Hazdra, J. Vobecký, H. Dorschner, K. Brand, Microelectron. J. 35 (2004) 249.

[3] S.D. Brotherton, P. Bradley, J. Appl. Phys. 53 (1982) 5270.

[4] D. Silber, W.D. Novak, W. Wondrak, B. Thomas, H. Berg, Proc. IEDM'85,162.

[5] J. Lutz, Proc. EPE'97, 1502.

[6] P. Hazdra, V. Komarnitskyy, Microelectron. J. 37 (2006) 197.

[7] J. Vobecký, P. Hazdra, IEEE Trans. Electron Devices 54 (2007) 1521.

[8] J. Vobecký, P. Hazdra, IEEE Electron Device Lett. 26 (2005) 873.

[9] J. Vobecký, P. Hazdra, IEEE Electron Device Lett. 23 (2002) 392.

[10] C. Claeys, E.Simoen, Radiation effects in advanced semiconductor materials and devices, Springer-Verlag Berlin, 2002.

[11] P. Hazdra, V. Komarnitskyy, IET Circuits, Devices Syst.1 (2007) 321.

[12] P. Hazdra, V. V. Komarnitskyy, Solid State Phenomena 95-96 (2004) 387.

[13] P. Hazdra, J. Rubeš, J. Vobecký, Nucl. Instr. Meth. B 154 (1999) 207.

[14] E.V. Monakhov, A. Ulyashin, G. Alfieri, A. Kuznetsov, B.S. Avset, B.G. Svensson, Phys. Rev. B 69 (2004) 153202.

[15] J. Vobecký, P. Hazdra, J. Homola, IEEE Trans. Electron Devices 43 (1996) 2283.

[16] P. Hazdra, V. Komarnitskyy, Mater. Sci. Eng. B, 159-160C (2009) 346.

[17] P. Hazdra, J. Vobecký, Solid-State Electron. 37 (1994) 127.

[18] J. Vobecký, P. Hazdra, V. Záhlava, Microelectron. Reliab. 43 (2003) 537.

[19] J. Vobecký, Hazdra P., O. Humbel, N. Galster, Microelectron. Reliab., 40 (2000) 427.

[20] J. Vobecký, P. Hazdra, V. Záhlava, Microelectron. J. 30 (1999) 513.

[21] P. Hazdra, K. Brand, J. Rubeš, J. Vobecký, Microelectron. J. 32 (2001) 449.

[22] J. Vobecký, P. Hazdra, V. Záhlava, Microelectron. J. 30 (1999) 513.

[23] N. Galster, M. Frecker, E. Caroll, J. Vobecký, P. Hazdra, Proc. PCIM INTER' 98, p. 69.

[24] P. Hazdra, J. Vobecký, N. Galster, O. Humbel, T. Dalibor Proc. ISPSD'2000, p. 123.

[25] P. Hazdra, J. Vobecký, Mater. Sci. Eng. B 124-125 (2005) 275.

[26] P. Pichler, Intrinsic point defects, impurities, and their diffusion in silicon, Springer-Verlag Wien, 2004.

[27] D.C. Schmidt, B.G. Svensson, S. Godey, E. Ntsoenzok, J.F. Barbot, C. Blanchard, Appl. Phys. Lett. 74 (1999) 3329.

[28] D. Bimberg, Semiconductor Nanostructures, Springer-Verlag Berlin, 2008.

[29] K. Barnham, D. Vvedensky, Low-dimensional semiconductor structures, Cambridge University Press, 2001.

[30] http://www.wsi.tu-muenchen.de/nextnano3

[31] P. Hazdra, J. Voves, E. Hulicius, J. Pangrác, Z. Šourek, Appl. Surf. Sci. 253 (2006) 85.

[32] G. Constantini, A. Rastelli, C. Manzano, P. Acosta-Diaz, R. Songmuang, G. Katsaros, O.G. Schmidt, K. Kern, Phys. Rev. Lett. 96 (2006) 226106.

[33] V.M. Ustinov, A.Y. Egorov, V.A. Odnoblyudov, N.V. Kryzhanovskaya, Y.G. Musikhin, A.F. Tsatsulnikov, Z.I. Alferov, J. Cryst. Growth 251 (2003) 388.

[34] Z. Mi, P. Bhattacharya IEEE J. Sel. Topics Quantum Electron. 14 (2008) 1171.

[35] T. Fukuda, J. Tatebayashi, M. Nishioka, Y. Arakawa, Proc. 27th Int. Conf. on the Physics of Semicond. 2005, p. 655.

[36] P. Hazdra, J. Oswald, V. Komarnitskyy, K. Kuldová, A. Hospodková, E. Hulicius, J. Pangrác, Superlattices and Microstructures 46 (2009) 324.

[37] P. Hazdra, J. Oswald, M. Atef, K. Kuldová, A. Hospodková, E. Hulicius, J. Pangrác, Materials Sci. Eng. B 147 (2008) 175.

[38] R. Songmuang, S. Kiravattaya, O.G. Schnidt, J. Cryst. Growth 249 (2003) 416.

[39] J.M. Ulloa, I.W.D. Drouzas, P.M. Koenraad, D.J. Mowbray, M.J. Steer, H.Y. Liu, M. Hopkinson, Appl. Phys. Lett. 90 (2007) 213105.

[40] A. Hospodková, E. Hulicius, J. Pangrác, J. Oswald, J. Vyskočil, K. Kuldová, T. Šimeček, P. Hazdra, O. Caha, J. Cryst. Growth (2009) submitted.

CURRICULUM VITAE

doc. Ing. Pavel Hazdra, CSc.

Date and Place of Birth:

April 21, 1960 in Prague, Czech Republic

University and Scientific Degrees:

1984, MSc. (Ing.),	Microelectronics, FEE CTU Prague
1991, PhD. (CSc.),	Microelectronics, FEE CTU Prague
1996, Associate Professor (doc.),	Electronics, FEE CTU Prague

Professional Career:

Assistant Professor, Dept. of Microelectronics FEE CTU Prague (1987-1996)

Associate Professor, Dept. of Microelectronics FEE CTU Prague (since 1996)

Head, Electron Device Research Group, Department of Microelectronics FEE CTU Prague (since 1992)

Vice-Dean for PhD studies and research, FEE CTU Prague (2006-2007)

Deputy-Dean FEE CTU Prague (2006-2007)

Visiting Positions:

University of Surrey, Guilford(UK), visiting research fellow (1988)

University of Hull, Hull(UK), visiting research fellow (1992)

University of Lund, Lund(S), visiting research fellow (1993-1994, 1996, 1997)

Research Interests:

Radiation defects in semiconductors, Ion implantation, Nanostructures and their characterization, Electrical and optical methods for characterization of deep levels in semiconductors, Programmable logical devices

University Courses:

Synthesis of integrated electronics systems, Design of programmable integrated circuits, Integrated circuits design, Programmable devices, Structures and technologies of microelectronics, Microelectronics, Semiconductor elements

Projects Coordination:

Impact of Capping Layers on Electronic States in Quantum Dots (GACR 202/09/0676) , Engineering of Quantum Dots (GACR 202/06/0718), Mechanism of Radiative Recombination in Subnanometer InAs/GaAs Laser Structures (GAAV IAA10103180), Accurate Control of Recombination Centre Introduction in Silicon (5. RP EU HPRI-1999-00039/72), Innovation of Education of Integrated Electronic Systems Design (FRVŠ 886/2006), Innovation of Education of Programmable Logical Devices (FRVŠ 2198/2002), coordinator of 6 CTU grants (1991-1999)

Coordinator of industrial projects with ABB Switzerland, Semiconductors, Freescale Semiconducteurs, France, Freescale Semiconductors, UK

Publications and Citations:

54 scientific papers in refereed journals (44 are excerpted in SCI Expanded)

135 contributions in proceedings of scientific conferences

2 patents

60 other technical and educational works

>300 citations in foreign scientific literature (120 in SCI Expanded)

h-index: 8 (ISI WoS), 10 (SCOPUS)

Professional Societies, Boards and Committees:

IEEE (Senior Member), American Physical Society, European Materials Science Society, Union of Czech Mathematicians and Physicists

Czechoslovakia Section IEEE – Committee member (2003 – 2006), MTT/AP/ED/EMC Joint Chapter – chairman (2003 – 2006), vice-chairman (2001 – 2003 and since 2006)

Program Committee of conferences POSTER (since 2006, vice-chairman 2006-7)

Organizing Committees of conferences: POSTER (1997-2002) – chairman, WORKSHOP (1995-2002), Testing of Integrated Circuits (1989), COMITE (2005)

Advising Board of the PhD Program "Electronics and Informatics" FEE CTU Prague (2006-2009, chairman 2006-2008)

Scientific Council, FEE CTU Prague (2006-2008)

Awards and Distinctions:

Medal of the Czech Ministry of Education, Youth and Sports, II. class (2003)

European Materials Society (E-MRS) Awards for the best poster presentation during E-MRS Spring Meetings 2007 and 2006

IEEE, Chairman of "The Chapter of the Year 2005" of the Region 8

IEEE, The Certificate of Appreciation by MTT/AP/ED/EMC Societies (2007)

MOTOROLA Award for contribution in microcontroller characterization (1998)

IEEE, The Acknowledgement of The MTT Society (2004)

The Acknowledgement of the dean of FEE CTU Prague for significant contribution to research in the branch of Electronics (1995)

CEI/Elsevier Award for the best poster presented on the conference Ion Implantation Technology (1990)

Selected Publications:

P. Hazdra, J. Oswald, V. Komarnitskyy, K. Kuldová, A. Hospodková, E. Hulicius, J. Pangrác, *"Influence of capping layer thickness on electronic states in self assembled MOVPE grown InAs quantum dots in GaAs"*, Superlattices and Microstructures, 46, 2009, pp. 324-327.

P. Hazdra, V. Komarnitskyy, *"Hydrogenation of Platinum Introduced in Silicon by Radiation Enhanced Diffusion"*, Materials Science and Engineering B, 159-160C, 2009, pp. 342-345.

P. Hazdra, V. Komarnitskyy, *"Influence of Radiation Defects on Formation of Thermal Donors in Silicon Irradiated with High Energy Helium Ions"*, Materials Science and Engineering B, 159-160C, 2009, pp. 346-349.

J. Vobecký, **P. Hazdra**, *"Dynamic avalanche in diodes with local lifetime control by means of palladium"*, Microelectronics Journal, vol. 39, 2008, pp. 878-883.

P. Hazdra, J. Oswald, M. Atef, K. Kuldová, A. Hospodková, E. Hulicius, J. Pangrác, *"InAs/GaAs quantum dot structures covered by InGaAs strain reducing layer characterised by photomodulated reflectance"*, Materials Science and Engineering B, vol. 147(2-3), 2008, pp. 175-178.

P. Hazdra, J. Voves, J. Oswald, K. Kuldová, A. Hospodková, E. Hulicius, J. Pangrác, *"Optical Characterisation of MOVPE Grown Vertically Correlated InAs/GaAs Quantum Dots"*, Microelectronics Journal 39, 2008, pp. 1070-1074.

P. Hazdra, V. Komarnitskyy, *"Local Lifetime Control in Silicon Power Diode by Ion Irradiation: Introduction and Stability of Shallow Donors"*, IET Circuits, Devices and Systems, vol 1 (5), 2007, pp. 321-326.

J. Vobecký, **P. Hazdra**, *"Radiation-Enhanced Diffuision of Palladium for a Local Lifetime Control in Power Devices"*, IEEE Transaction on Electron Devices, vol. 54(6), 2007, pp. 1521-1526.

P. Hazdra, J. Voves, E. Hulicius, J. Pangrác, Z. Šourek, *"Ultrathin InAs and Modulated InGaAs Layers in GaAs Grown by MOVPE Studied by Photomodulated Reflectance Spectroscopy"*, Applied Surface Science, Vol. 253/1, 2006, pp 85-89.

P. Hazdra, V. Komarnitskyy,*"Lifetime control in silicon power P-i-N diode by ion irradiation: suppression of undesired leakage"*, Microelectronics Journal , Vols. 37/3, 2006, pp.197-203.

P. Hazdra, J. Vobecký,*"Platinum in-diffusion controlled by radiation defects for advanced lifetime control in high power silicon devices"*, Materials Science and Engineering: B, Vols. 124-125, 2005, pp. 275-279.

J. Vobecký, **P. Hazdra,** *"High-Power P-i-N Diode With Local Lifetime Control Using Palladium Diffusion Controlled by Radiation Defects"*, IEEE Electron Device Letters 26(12) , 2005, pp. 873-875.

P. Hazdra, J. Vobecký, *"Radiation enhanced diffusion of implanted platinum in silicon guided by helium co-implantation for arbitrary control of platinum profile"*, Nuclear Instruments and Methods in Physics Research B 230(1-4), 2005, pp. 225-229.

P. Hazdra, J. Vobecký, H. Dorschner, K. Brand, *"Axial lifetime control in silicon power diodes by irradiation with protons, alphas, low- and high-energy electrons"*, Microelectronics Journal, vol. 35(2004), pp 249-257.

J. Vobecký, **P. Hazdra**,*"Advanced Local Lifetime Control for Higher Reliability of Power Devices*, Microelectronics Reliability, 43(2003), 1883-1888.

J. Vobecký, **P. Hazdra**, V. Záhlava, *"Impact of the electron, proton and helium irradiation on the forward I-V characteristics of high-power P-i-N diode"*, Microelectronics Reliability 439(2003), pp. 537-544.

P. Hazdra,H. Dorschner, *"Radiation defect distribution in silicon irradiated with 600 keV electrons"*, Nuclear Instruments and Methods in Physics Research B 201(3), 2003, pp. 513 - 519.

J. Vobecký, **P. Hazdra**, *"Helium irradiated high-power P-i-N diode with low ON-state voltage drop"*, Solid-State Electronics, 47(1), 2003, pp. 45-50.

P. Hazdra, J. Voves, J. Oswald, E. Hulicius, J. Pangrác, T. Šimeček, "*InAs δ-layer structures in GaAs grown by MOVPE and characterised by luminescence and photocurrent spectroscopy"*, Journal of Crystal Growth, 248C, 2003, pp. 328-332.

P. Hazdra, K. Brand, J. Vobecký, *"Defect distribution in MeV proton irradiated silicon measured by high-voltage current transient spectroscopy*", Nuclear Instruments and Methods in Physics Research B 192(3), 2002, pp. 291-300.

J. Vobecký, **P. Hazdra**, *"High-power P-i-N Diode With the Local lifetime Control Based on the Proximity Gettering of Platinum*", IEEE Electron Device Letters, 23(7), 2002, pp. 392-394

P. Hazdra, J. Vobecký, K. Brand, *"Optimum lifetime structuring in silicon power diodes by means of various irradiation techniques"*, Nuclear Instruments and Methods in Physics Research B 186(1-4), 2002, pp. 414 - 418.

P. Hazdra, K. Brand, J. Rubeš, J. Vobecký, *"Local lifetime control by light ion irradiation: impact on blocking capability of power P-i-N diode"*, Microelectronics Journal, 32(56), 2001, pp. 449 - 456.

P. Hazdra, J. Rubeš, J. Vobecký, *" Divacancy profiles in MeV helium irradiated silicon from reverse I-V measurement"*, Nuclear Instruments and Methods in Physics Research, B 154(4), 1999, pp. 207-217.

Vobecký J., **Hazdra P.** , Záhlava V., *"Open circuit voltage decay lifetime of ion irradiated devices"*, Microelectronics Journal, 30(6), 1999, pp. 513 - 520.

P. Tidlund, M. Kleverman, **P. Hazdra**, *"Excitation spectrum of a PtLi-related center in silicon"*, Physical Review B, 59(7), 1999, pp. 4858 - 4863.

P. Hazdra, J. Vobecký : *"Application of High Energy Ion Beams for Local Lifetime Control in Silicon"*, Material Science Forum 248-249, 1997, pp. 225-228.

J. Vobecký, **P. Hazdra**, J. Homola, *"Optimization of Power Diode Characteristic by Mean of Ion Irradiation"*, IEEE Transactions on Electron Devices, Vol. 43, no.12, 1996, pp. 2283-2289.

P. Hazdra, D. Sands, D.J. Reeve, *"Origin of Defect States at ZnS/Si Interfaces"* Applied Physics, A61, 1995, pp. 637-641

P. Hazdra, V. Hašlar, J. Vobecký, *"Application of Defect Related Generation Current for Low-Dose Ion Implantation Monitoring"*, Nuclear Instruments and Methods in Physics research, B96, (1-2), 1995, pp. 104-108.

P. Hazdra, J. Vobecký, *"Accurate simulation of fast ion irradiated power devices"*, Solid-State Electronics, Vol. 37, No. 1, 1994, pp. 127-134.

P. Hazdra, V. Hašlar, M. Bartoš, *"The influence of implantation temperature and subsequent annealing on residual implantation defects in silicon"*, Nuclear Instruments and Methods in Physics Research, B55, 1991, pp. 637-641.